Electronic Supplementary Information (ESI)

Fabrication of $Cd_{0.5}Zn_{0.5}S$:Cu QDs incorporated organically modified SiO_2 films showing entire visible colour emission with high quantum yield†

Manish Kr Mishra and Goutam De*

Nano-Structured Materials Division, CSIR–Central Glass and Ceramic Research Institute, 196, Raja S. C. Mullick Road, Kolkata 700032 (India). E-mail: gde@cgcri.res.in

1. Experimental section

1.1 Materials. Cadmium acetate dihydrate, $Cd(OOCCH_3)_2 \cdot 2H_2O$ (98%), Thiourea (AR) were purchased from Merck (India) Ltd., n-butanol and methanol (AR) from Rankem Ltd. (India), Aluminium acetylacetonate ($Al(acac)_3$) was supplied by Lancaster, zinc acetate dihydrate $Zn(OOCCH_3)_2 \cdot 2H_2O$ (98 %), tetraethylorthosilicate (TEOS), (3-Glycidyloxypropyl)-trimethoxy silane (GLYMO) (98 %) and pluronic P123 (EO70PO20EO70; M_{av} = 5800) were purchased from Sigma Aldrich. Water (18 MΩ) used for hydrolysis was obtained from Milli-Q System (Millipore) and soda-lime glass slides for coating deposition were purchased from Reviera.

1.2 Preparation of organically modified silica hybrid (ORMOSIL) sols and films

In order to prepare the hybrid (ORMOSIL) sol,[22] 2.33:1 molar ratio of TEOS and GLYMO has been taken in a round bottom flask containing 21 g of n-butanol and stirred for proper mixing. To this, a mixture of catalytic amount of acid (0.586 g), water (10.9 g) and methanol (1.43 g) was added and stirred for next 30 min. The above resultant mixture was refluxed at 80 °C for 90 min and allowed to cool at room temperature. The sol obtained was aged for 2 h in closed condition at room temperature. $Al(acac)_3$ (0.02 mol per mol of GLYMO) was then added and stirred until it get dissolved for initiating the epoxy polymerization. The sol was aged for 24 h in refrigerator (± 5 °C) prior to use. The final equivalent SiO_2 content of the sol was 21 wt%.

In the next step for the synthesis of fluorescent $Cd_{0.5}Zn_{0.5}S$:Cu NPs incorporated transparent ORMOSIL films, first micellar solution of P123 (1.7×10^{-4} mol) with 3 g MeOH was prepared through constant stirring for 30 min. Separately $Cd(ac)_2 \cdot 2H_2O$, $Zn(ac)_2 \cdot 2H_2O$ and thiourea were magnetically blended in 7 g MeOH for 30 min to obtain Zn/Cd acetate/thiourea complex solution. For the doping of Cu-ion, different amounts of $Cu(ac)_2 \cdot H_2O$ were mixed in the above complex solution. In the next step, complex solutions were mixed with methanolic solution of P123 micelles to obtain complex incorporated P123 miceller solutions. Finally 10 g ORMOSIL sol was added to the final mixture solution to obtain clear sol. Due to the presence of cu^{2+} ion, sols acquired a faint bluish coloration. Dip coatings were performed using these clear sols on soda-lime glass substrates with a withdrawal speed of 21 cm min^{-1}. Coated films were completely transparent and visually colourless after drying at 60 °C (for 1h). After the heat treatment at 185 °C for 10 min the colour of the films changes to bright yellow (except Cd_0ZnS), while maintaining their transparency. These films have been further cured at 90 °C for another 1h. Exact molar concentrations of ingredients used are given in the Table S1.

Table S1 Nominal composition of the Zn, Cd, Cu salts and thiourea (TU) used to prepare different sols. The molar compositions along with equivalent SiO_2 content of the sols are also given.

Sample name (Fluorescent colour)	**$Zn(ac)_2 \cdot 2H_2O$ (mol)**	**$Cd(ac)_2 \cdot 2H_2O$ (mol)**	**$Cu(ac)_2 \cdot H_2O$ (mol)**	**TU (mol)**	**Equivalent SiO_2 in sols (mol)**
Cd_0ZnS ORMOSIL film (Blue)	0.01822	0	0	0.01822	0.03471
$Cd_{0.5}Zn_{0.5}S$ ORMOSIL film (Cyan)	0.00911	0.00911	0	0.01822	0.03471
$Cd_{0.5}Zn_{0.5}S:Cu$ ORMOSIL film (Yellow)	0.00911	0.00911	0.000150	0.01822	0.03471
$Cd_{0.5}Zn_{0.5}S:Cu$ ORMOSIL film (Orange)	0.00911	0.00911	0.000508	0.01822	0.03471
$Cd_{0.5}Zn_{0.5}S:Cu$ ORMOSIL film (Red)	0.00911	0.00911	0.00150	0.01822	0.03471

1.3 Characterization

UV-Visible absorption and emission spectra of the films were recorded with Cary 50, Varian Inc and PTI QM-30 spectrometers, respectively. Fourier transformed infrared (FTIR) absorption spectra of the film samples deposited on Si wafer were recorded using a Nicolet 380 FTIR spectrometer. High angle XRD measurements of the films were performed with a Rigaku SmartLab X-ray diffractometer operating at 9 kW (200 mA; 45 kV) using Cu-Kα (λ= 1.5405 Å) radiation. Transmission electron microscopic (TEM) measurements were carried out with JEOL JEM 2100F operating at 200 kV. For this purpose small amount of scratched off films was ultrasonicated in MeOH and centrifuged for 5 times to remove surfactant and placed on a carbon coated Mo-grid and analyzed. In case of FESEM films were deposited on the single side polished silicon wafer and analysed by ZEISS SUPRA 35VP field-emission scanning electron microscope. EPR measurement was done at room temperature using JEOL (JS FA200) spectrophotometer operating at X-band frequency, 10 mW power and 9150.13 MHz microwave frequency. The range was 220-420 with 1 x 100 mT sweep width, 2 min sweep time, 1.4x10 amplitude, 0.03 time constant and 320 central field.

The luminescence decay measurements were performed by time correlated single-photon counting (TCSPC) method. For decay measurements, samples were excited at 375 nm using a picosecond diode laser (IBH Nanoled-07) at a repetition rate of 1 MHz. The typical FWHM of the system response is about 200 ps. The fluorescence decays were analyzed using IBH DAS6 software. The quality of fitting was evaluated from the χ^2 value and DW parameters and the PL decay curve are fitted using a triexponential function.

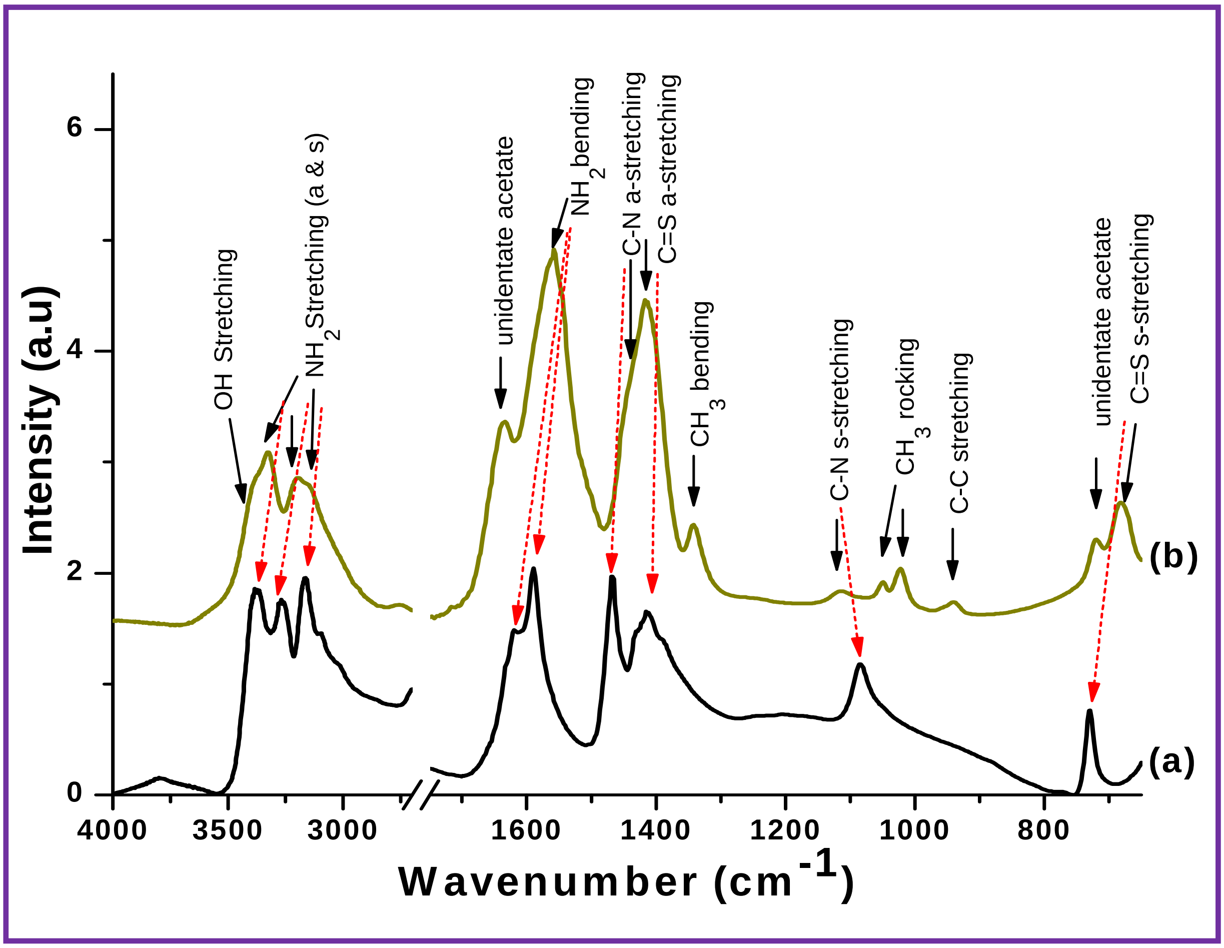

Fig. S1 FTIR spectra of (a) thiourea (TU) and (b) complex formed by TU with Cd(ac)$_2$ and Zn(ac)$_2$. The peak assignments are shown in the body of the figure as well as in Table S2.

Structure analysis of the complex by FTIR. As TU can bind metal ions from sulphur (S) or nitrogen (N) or from both ends, the FTIR studies reveal useful information regarding the formation of coordination bonds. Considering the shifting of C=S, C-N and NH$_2$ stretching frequencies, the nature of complex formation and a plausible structure of complex can be predicted.[25,26] Decrease in C=S stretching frequency with concomitant increase in C-N stretching frequency should be observed when TU binds with metal ion via S-end or vice-versa if binds through N-end. In the present case we did not observe noticeable shift of C=S asym stretching compared to the uncoordinated TU (both the complex and uncoordinated TU absorbs at 1417 cm^{-1} (see Fig. S1a,b), however the corresponding C=S sym stretching peak significantly shifted from 732 cm^{-1} (uncoordinated TU; see Fig. S1a) to lower frequency at 680.2 cm^{-1} (in case of complex; see Fig. S1b and Table S2) after complex formation. This result indicates decrease of C=S bond strength due to the binding from S-end preferably with Cd^{2+} ion as it is more softer than Zn (soft-soft coordination). Again, TU peaks at 1472, 1590 and 1620 cm^{-1} (Fig. S1a) showed a noticeable down shift to lower frequency at 1450 and 1557 cm^{-1}, respectively after complex formation (Fig. S1b) indicating the binding of N-sites with metal ion (preferably with Zn^{2+} because of hard-hard combination). FTIR study is therefore indicates bidentate characteristics of TU. As we have used two different metal ions (1 mol each), one is relative hard (Zn) in nature than other (Cd) and 2 moles of TU it is obvious that TU will be bonded as a bridging bidentate where N- and S-sites will be bonded with Zn and Cd ions, respectively as shown in Fig. S2. Because of ligand (TU) deficiency acetate groups will also coordinate with the metal ions. Appearance of peaks at 1635 and 721.4 cm^{-1} in case of complex (Fig. S1b) supports presence of unidentate acetate anion. As Cd^{2+} ion prefers octahedral coordination, available water molecules will coordinate to serve this purpose. It is expected that these water molecules will remain H-bonded with the acetate originated C=O groups. Such H-bonding would cause shifting of OH vibrations towards lower frequency, and for this reason we are unable to resolve these absorptions due to the overlapping with NH_2 vibrations. Considering all these, the possible structure of the complex has been shown in Fig. S2.

Table S2 FTIR peak assignments corresponding to Figure S1.

Thiourea (cm^{-1})	**Complex formed by TU, $Cd(ac)_2$ and $Zn(ac)_2$ (cm^{-1})**	**Assignment**
732	680.2	C=S (sym Stretching)
------	721.4	Unidentate acetates
------	940	C-C stretching
------	1020	CH_3 (rocking)
------	1052	CH_3 (rocking)
1089	1113	C-N (sym Stretching)
------	1342	CH_3 (bending)
1417	1417.4	C=S (asym Stretching)
1472	1450	C-N (asym Stretching)
1590 , 1620	1557	NH_2 (Bending)
-------	1635	Unidentate acetate
3172	3143.5	NH_2 (sym Stretching)
3272	3204	NH_2 (asym Stretching)
3380	3327	NH_2 (asym Stretching)

‘sym’ and ‘asym’ stands for symmetric and asymmetric stretching, respectively.

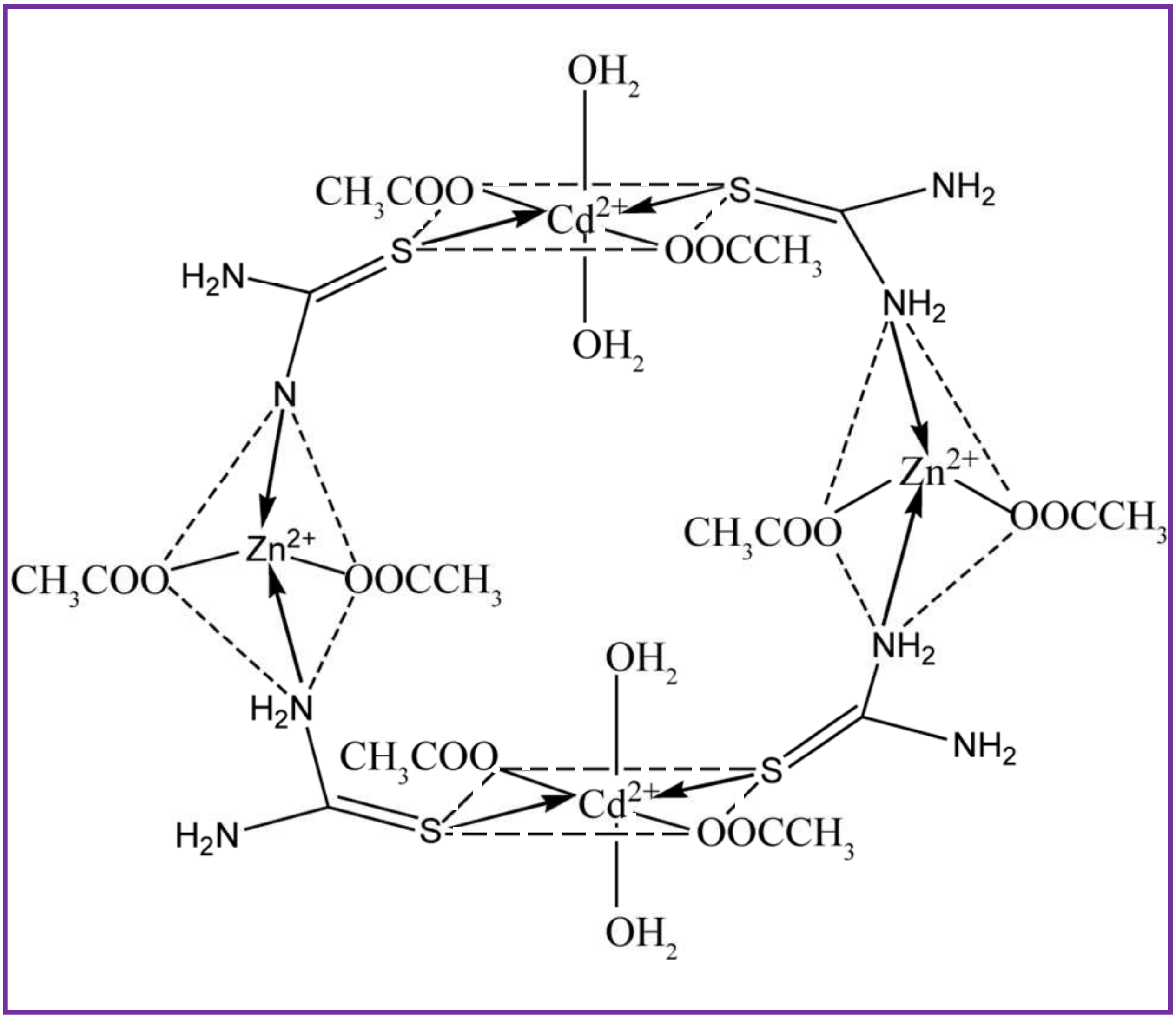

Fig. S2 Plausible structure of the complex [CdZn(ac)$_4$(SC((NH)$_2$)$_2$)$_2$(H$_2$O)$_2$]$_2$ formed by bidentate TU with zinc and cadmium acetates.

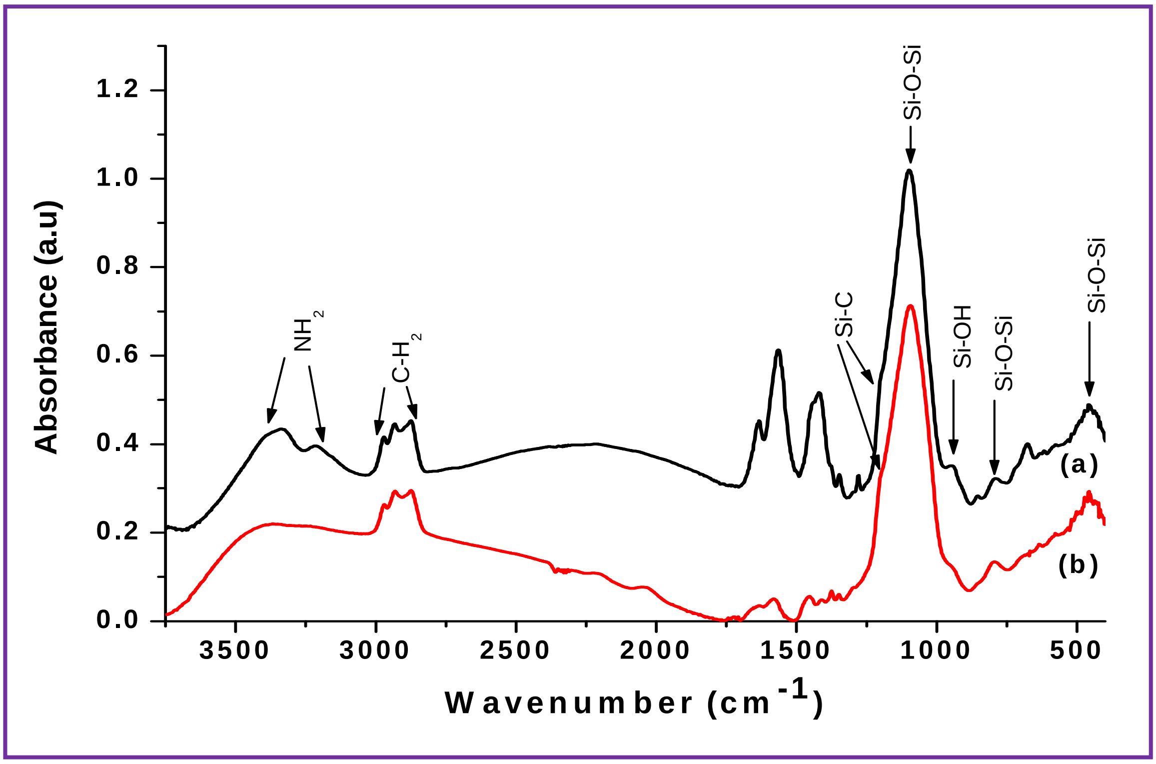

Fig. S3 FTIR spectra of (a) [$CdZn(ac)_4(SC((NH)_2)_2)_2(H_2O)_2$] complex inside ORMOSIL-P123 micelle, and (b) $Cd_{0.5}Zn_{0.5}S$/ORMOSIL-P123 film after decomposition of the complex at 185 °C. Peak assignments are given in the body of the figure. Absence of thiourea and acetate related peaks in case of (b) indicates the decomposition of complex to form $Cd_{0.5}Zn_{0.5}S$. Appearance of CH_2 and Si–C related peaks with similar intensity indicates the presence of ORMOSIL/P123 structure.

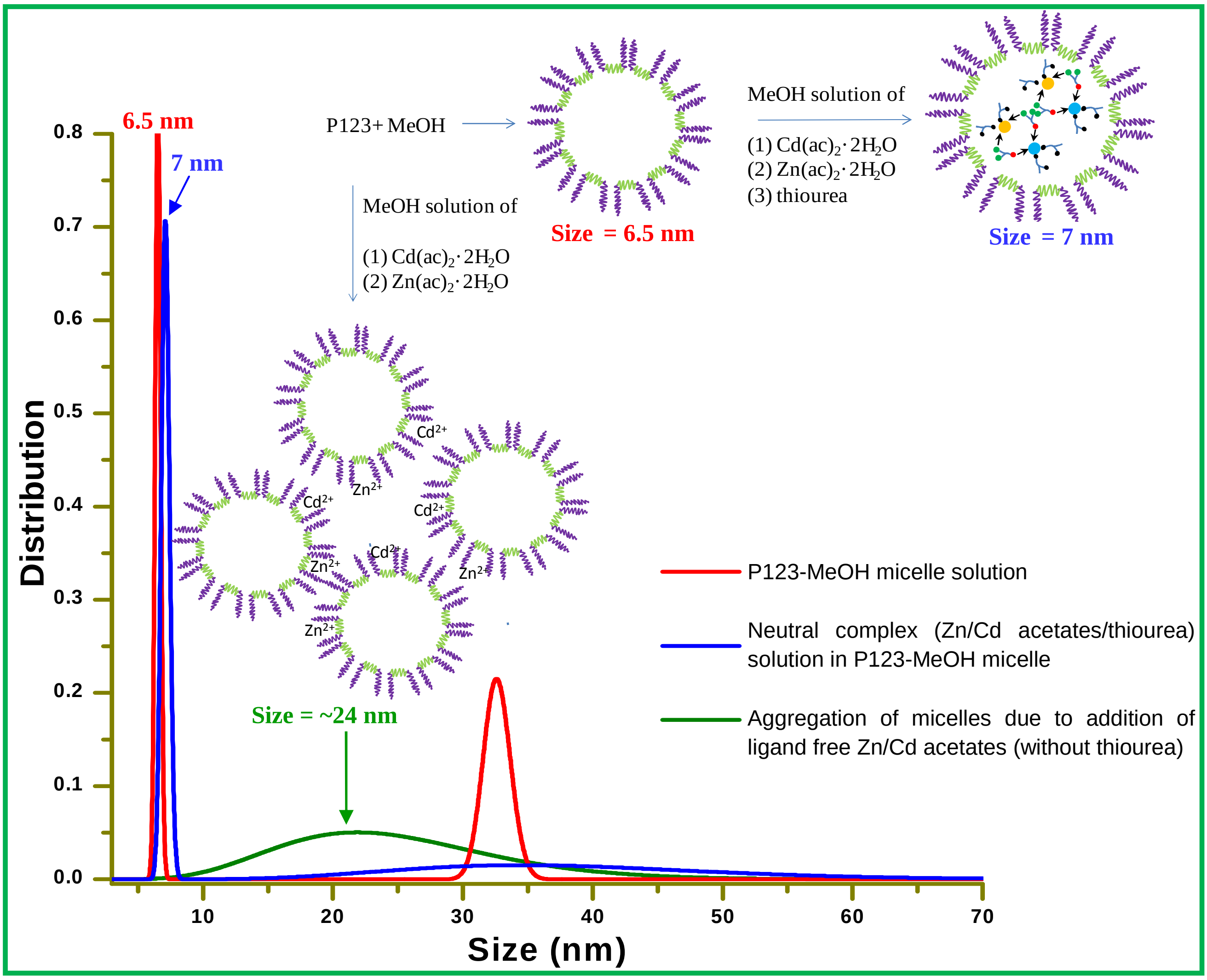

Fig. S4 SAXS profiles showing the size of micelles formed: (a) P123 in MeOH in absence of any ion or ligand (red curve), (b) in presence of neutral Zn/Cd-thiourea complex (blue curve) and (c) in presence of only metal ions without any ligand (green curve). Inset shows the size and expected micelle structures as observed by SAXS.

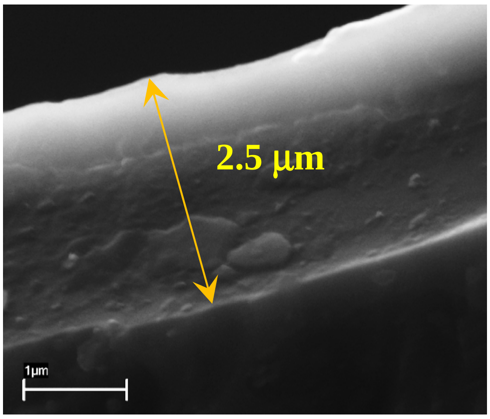

Fig. S5 FESEM cross-section image showing the thickness of $Cd_{0.5}Zn_{0.5}S$:Cu (0.000508 mol) ORMOSIL film on silicon (Si) substrate.

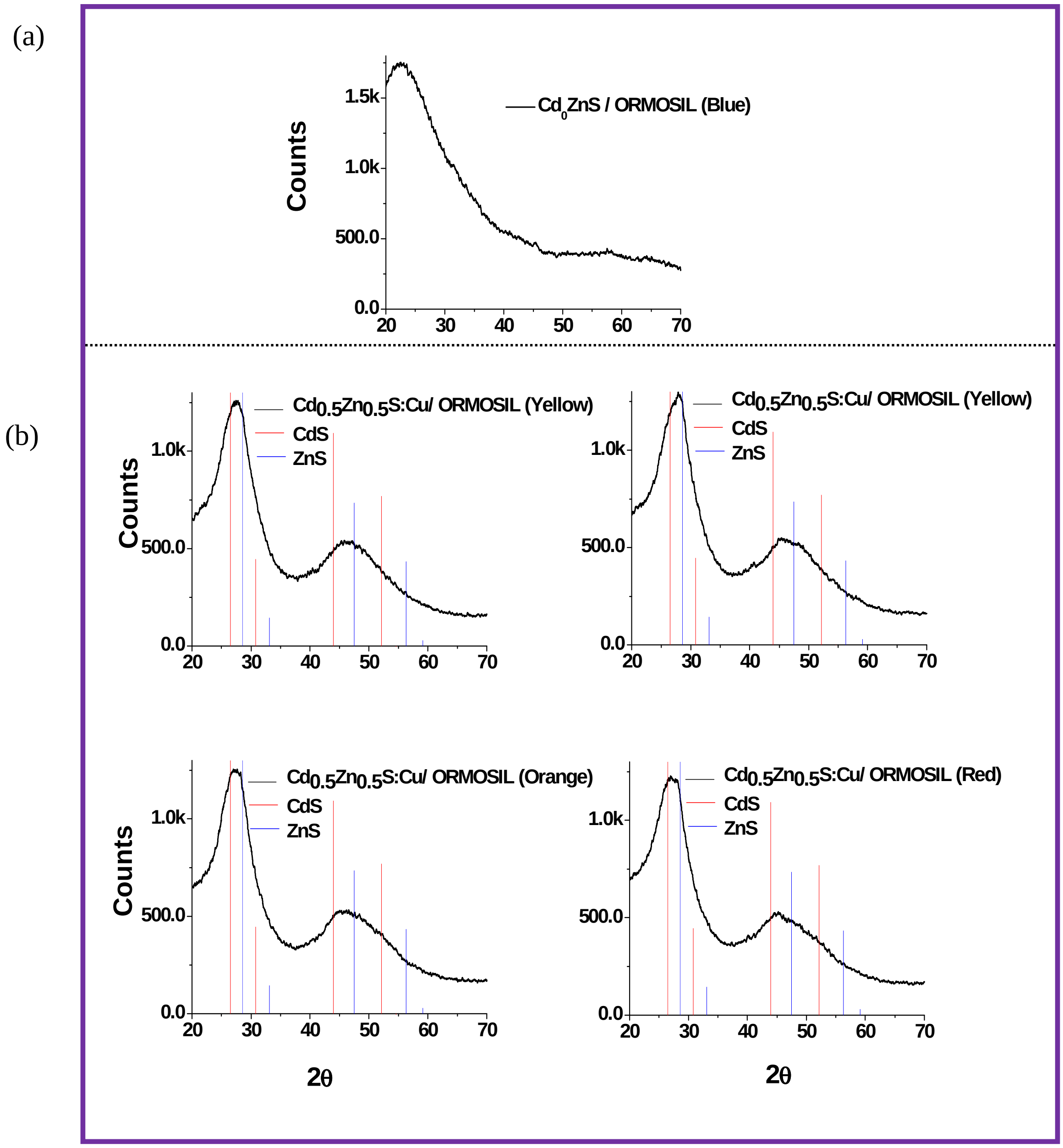

Fig. S6 XRD patterns of (a) Cd_0ZnS doped ORMOSIL film; (b) undoped $Cd_{0.5}Zn_{0.5}S$ (i), and 0.00015 mol (ii), 0.000508 mol (iii), 0.0015 mol (iv) Cu^{2+} ion doped $Cd_{0.5}Zn_{0.5}S$ ORMOSIL films.

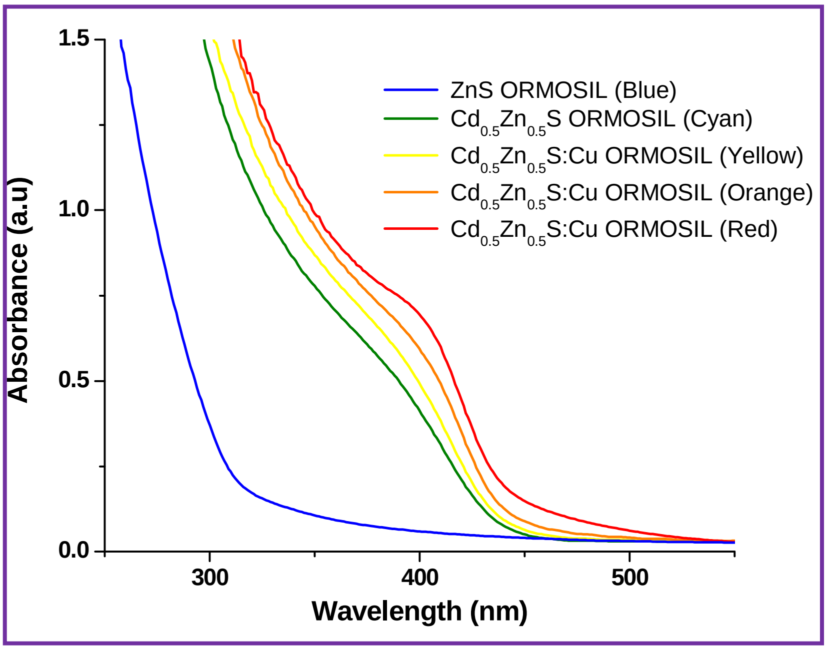

Fig. S7 UV-visible spectra of the films showing the change in absorption wavelength (λ_{max}) with incorporation of Cu^{2+} ions in Cd_0ZnS/ORMOSIL films.

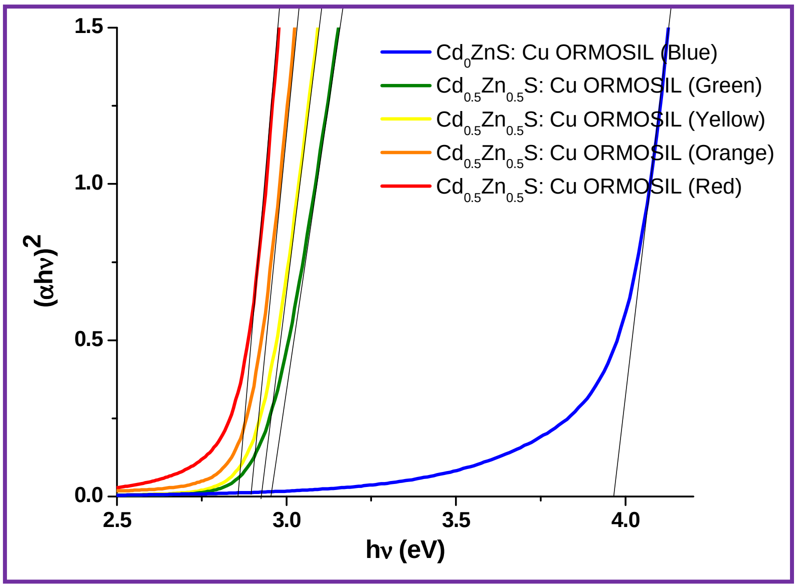

Fig. S8 $(\alpha h\nu)^2$ vs hν plots showing the band gap tuning (decrease in band-gap) with incorporation of Cu^{2+} ions.

Table S3 Calculated band gaps of different Cd$_0$ZnS and Cd$_{0.5}$Zn$_{0.5}$S/ORMOSIL films from $(\alpha h\nu)^2$ vs hν plot.

Name of the sample	**Band gap (eV)**
Cd$_0$ZnS ORMOSIL film (Blue)	3.9
Cd$_{0.5}$Zn$_{0.5}$S ORMOSIL film (Cyan)	2.95
Cd$_{0.5}$Zn$_{0.5}$S:Cu ORMOSIL film (Yellow)	2.92
Cd$_{0.5}$Zn$_{0.5}$S:Cu ORMOSIL film (Orange)	2.89
Cd$_{0.5}$Zn$_{0.5}$S:Cu ORMOSIL film (Red)	2.85

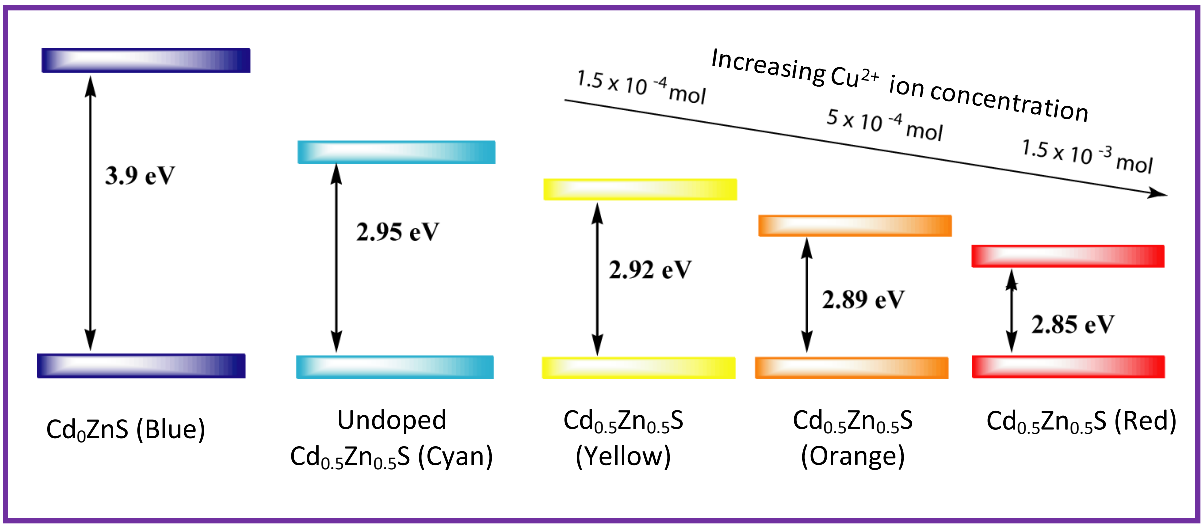

Fig. S9 Schematic illustration of the band-gap energy diagram of light emitting ORMOSIL films as shown in table S3.

Table S4 Relative quantum yield (QY) is measured with respect to 0.5 x 10^{-5} M aqueous rhodamin B solution. In order to minimize re-absorption effect, 0.5 x 10^{-5} M aqueous solution of rhodamin B has been used and films were prepared by reducing the actual concentration of the reactants (as tabulated in Table 1) by 1/10 factor. Relative QY was calculated using equation S1:

$$QY_{sample} = (F_{sample}/F_{ref})(A_{ref}/A_{sample})(n^2_{sample}/n^2_{ref}) * QY_{ref} \quad \text{......(eqn S1)}$$

Where,

F → Integrated area under the PL emission curve

A → Absorbance at excitation wavelength

n → Refractive index of the samples

QY_{sample} → Quantum yield of the sample

QY_{ref} → Quantum yield of the reference (here rhodamin B)

Sample name	**Absorbance at excitation wavelength (365 nm)**	**Integrated emission area**	**Refractive index of the medium**	**Quantum yield**
0.5x 10^{-5} M Rhodamin B (in H_2O)	0.0447	461.61	(H_2O)= 1.33	0.31
Cd_0ZnS ORMOSIL film (Blue)	0.0154	250.56	SiO_2 /P123 Film = 1.495	0.61
$Cd_{0.5}Zn_{0.5}S$ ORMOSIL film (Cyan)	0.073	1470.025	SiO_2 /P123 Film = 1.495	0.76
$Cd_{0.5}Zn_{0.5}S$: Cu ORMOSIL film (Yellow)	0.084	1417.59	SiO_2 /P123 Film = 1.495	0.64
$Cd_{0.5}Zn_{0.5}S$:Cu ORMOSIL film (Orange)	0.09	1092.68	SiO_2 /P123 Film = 1.495	0.41
$Cd_{0.5}Zn_{0.5}S$: Cu ORMOSIL film (Red)	0.0955	995.92	SiO_2 /P123 Film = 1.495	0.39

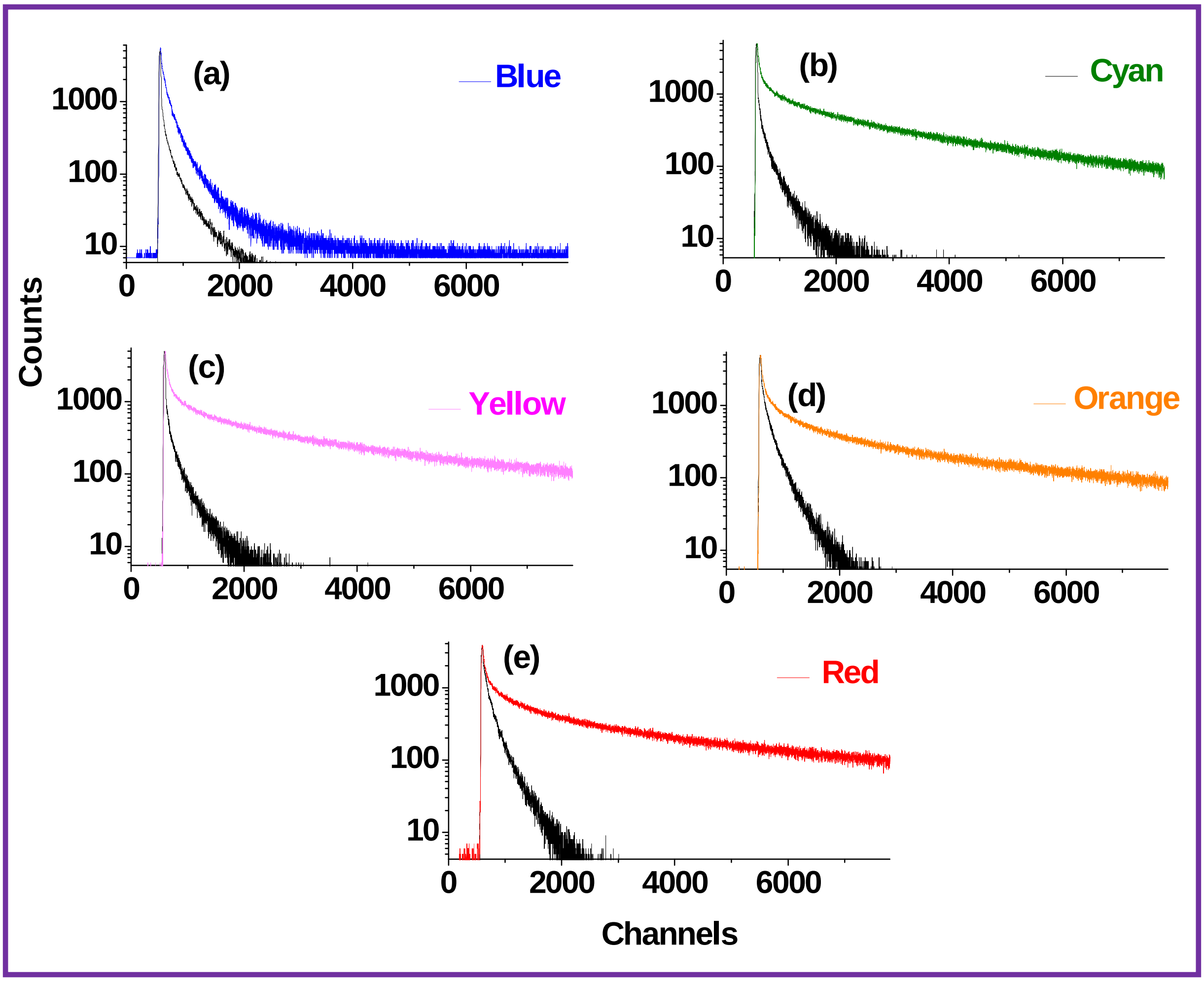

Fig. S10 PL decay curves of (a) Cd_0ZnS, (b) undoped $Cd_{0.5}Zn_{0.5}S$, and (c) 0.00015 mol (d) 0.0005 mol and (e) 0.0015 mol Cu^{2+} doped $Cd_{0.5}Zn_{0.5}S$ ORMOSIL films, measured at emission wavelength of 435, 500, 550, 585 and 625 nm, respectively. Excitation was done with 375 nm nano LED.

Table S5 Calculated average lifetime (from fitting data) of different $Cd_{0.5}Zn_{0.5}S$:Cu and Cd_0ZnS doped ORMOSIL films.

Sample name	**Decay time τ_{av}(ns)**	χ^2
Cd_0ZnS ORMOSIL film(Blue)	25.09	1.289
$Cd_{0.5}Zn_{0.5}S$:Cu ORMOSIL film (Cyan)	52.187	0.974
$Cd_{0.5}Zn_{0.5}S$:Cu ORMOSIL film (Yellow)	51.62	1.089
$Cd_{0.5}Zn_{0.5}S$:Cu ORMOSIL film(Orange)	51.028	1.111
$Cd_{0.5}Zn_{0.5}S$:Cu ORMOSIL film (Red)	50.127	1.098

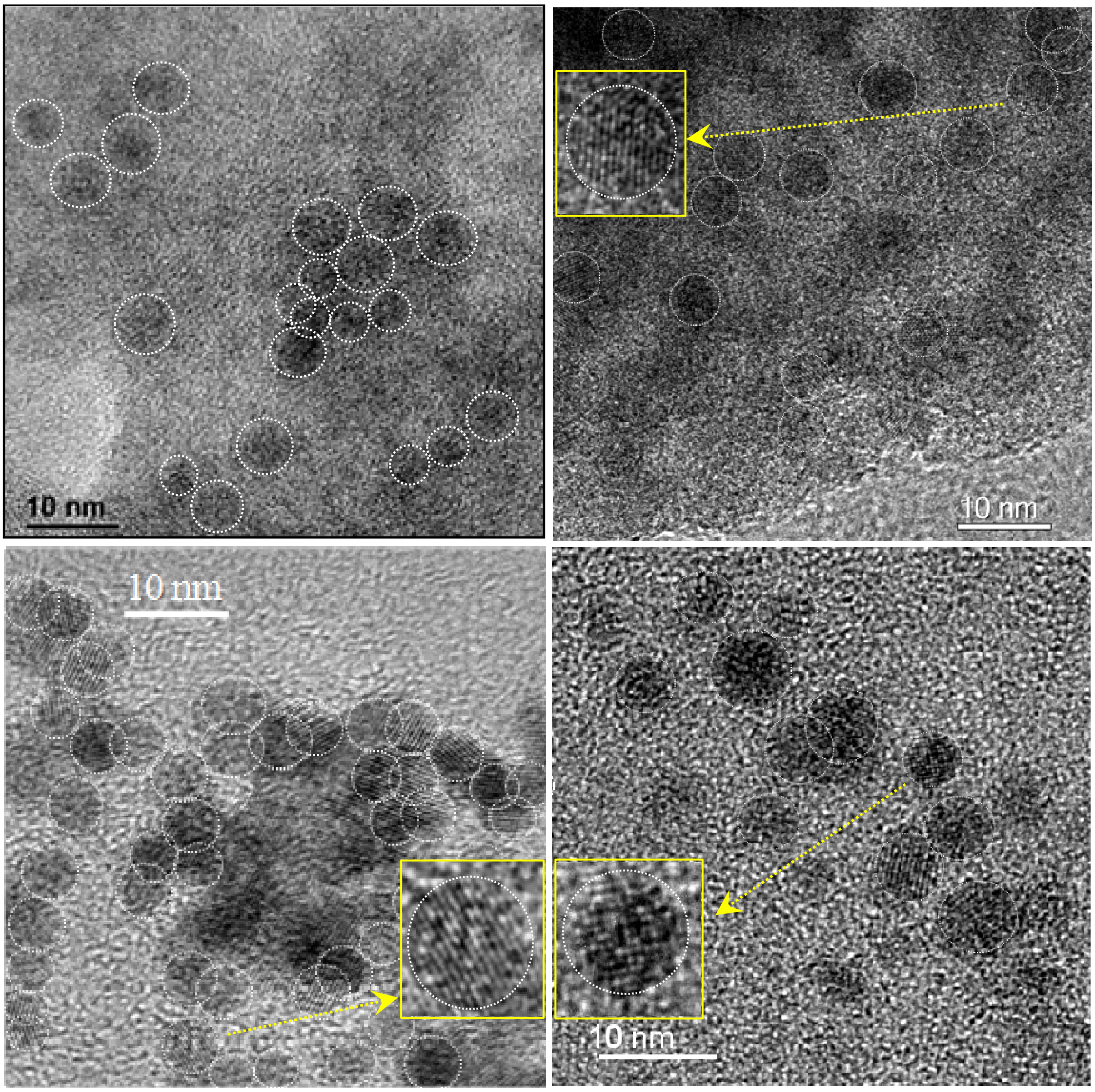

Fig. 11 HR-TEM images of (a) Cd_0ZnS, (b) undoped $Cd_{0.5}Zn_{0.5}S$, and (c) 0.00015 mol and (d) 0.0015 mol Cu^{2+} doped $Cd_{0.5}Zn_{0.5}S$ ORMOSIL film samples.

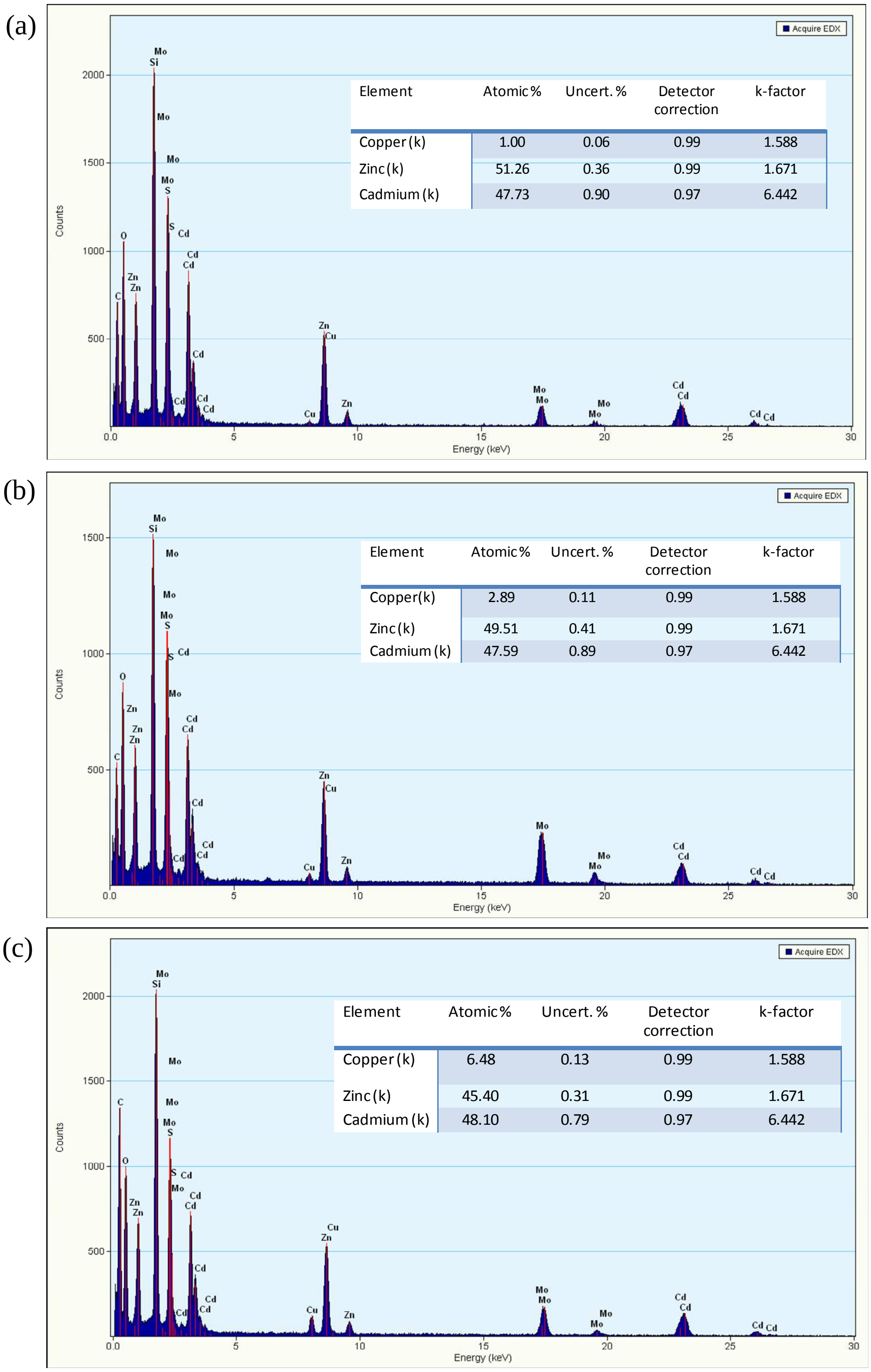

(a)

Element	Atomic %	Uncert. %	Detector correction	k-factor
Copper (k)	1.00	0.06	0.99	1.588
Zinc (k)	51.26	0.36	0.99	1.671
Cadmium (k)	47.73	0.90	0.97	6.442

(b)

Element	Atomic %	Uncert. %	Detector correction	k-factor
Copper(k)	2.89	0.11	0.99	1.588
Zinc (k)	49.51	0.41	0.99	1.671
Cadmium (k)	47.59	0.89	0.97	6.442

(c)

Element	Atomic %	Uncert. %	Detector correction	k-factor
Copper (k)	6.48	0.13	0.99	1.588
Zinc (k)	45.40	0.31	0.99	1.671
Cadmium (k)	48.10	0.79	0.97	6.442

Fig. S12 EDS spectra of 0.00015 mol (a), 0.000508, and 0.0015 mol (c) Cu-ion doped $Cd_{0.5}Zn_{0.5}S$ ORMOSIL film samples showing the atomic % of Cu with respect to the total concentration of the Zn and Cd obtained from TEM analysis.